CHARA Technical Report

No. 86 1 August 2000

Imaging and Fourier Coverage: Mapping with Depleted Arrays

P.G. Tuthill and J.D. Monnier

1. INTRODUCTION

In the consideration of the design of a sparse-pupil imaging system, such as an earth-rotation synthesis interferometer, a particularly interesting question arises. How much Fourier coverage do I need to make images of my targets?

The question is a surprisingly difficult one to answer. Part of the problem lies in the multi-dimensional space which needs to be explored. Rules of thumb have long been used by radio astronomers. "The number of Fourier data obtained should equal the number of pixels in the map". And of course, it is important to match the resolution of the instrument to the spatial scales of the object to be mapped: short baselines for extended structure, long for compact features. We will come to these again later on.

Another great difficulty with the mapping question arises from the signal-to-noise of the data points. When processed through current imaging software, the signal-to-noise of data has been found to be crucial in obtaining reliable maps. Many thousands of data points at low signal-to-noise (significantly less than 1) may fail to converge to anything usable, while only a handful of good data-points may reveal reliable image structure.

What is needed is a study encompassing a range of different target images with structure on various spatial scales, with simulated observations on a range of different Fourier synthesis arrays at a range of different signal-to-noise levels. Unfortunately, this is not that study. Work of this nature has been performed, often associated with the commissioning of a new radio-telescope, and usually using simulated datasets.

What we have done is to work with real Fourier synthesis data from an optical aperture masking interferometry experiment performed at the Keck I telescope. Extensive details of the experimental setup and data reduction methods can be found in Tuthill et al., *PASP* 2000 **112,** 555. Choosing data sets known to produce good, reliable maps, we have successively "depleted" the imaging arrays by discarding (in software) more and more of the array elements. Note that this has two distinct detrimental effects on the imaging. The Fourier coverage is more sparse, so that the algorithm has to interpolate over larger and larger gaps. The combined signal-to-noise of the total dataset is lower, as the algorithm has

[1]Center for High Angular Resolution Astronomy, Georgia State University, Atlanta GA 30303-3083
TEL: (404) 651-2932, FAX: (404) 651-1389, FTP: ftp.chara.gsu.edu, WWW: http://www.chara.gsu.edu.
Funding for the CHARA Array is provided by the National Science Foundation, the W. M. Keck Foundation, the David and Lucile Packard Foundation and by Georgia State University.

fewer points to average out the noise.

The Keck interferometry uses a single "snapshot" mode of operation. This presents a further difficulty when attempting to draw a comparison to, say, an earth-rotation synthesis device. In the snapshot mode, all Fourier data are found at fairly discrete spatial frequencies, and can be considered "independent". However, the question arises – how far should one consider an earth-rotation array rotate before it is measuring a significantly different spatial frequency? Clearly, the answer depends on the source structure on the sky.

However, for the present purposes, let us consider objects which are only just resolved, so that the visibilities do not change quickly with position angle. In such cases, we might imagine that over the course of a night, a rotation-synthesis interferometer is able to record the equivalent of a few – say three or four – separate and independent snapshots.

To take a concrete example, imagine a 7-element earth-rotation array. We have compiled, in Table 1, a listing of the quantity of visibility and independent closure phase data collected by an array of 3 – 36 elements. From this table, we find that a 7-element array has 21 baselines and 15 independent closure phases. Over the course of a night, we might argue, this array would generate 4× this or 84 visibilities and 60 closure phases. Looking again at Table 1, we find this is roughly equivalent to a snapshot array of around 13 or 14 elements. It will be useful to bear this in mind for later comparison.

2. STUDY 1: RANDOMLY DEPLETED ARRAY

The first experiment conducted utilized Fourier data of Wolf-Rayet 104, observed with an annular-shaped pupil and sampled as a 36-hole circular ring. The MEM-reconstructed map based on the full dataset, shown in Figure 1 part A, has noise features (not visible at the minimum contour shown) around the 0.25 – 0.5 % level. Moving on to Figure 1 part B, sidelobes due to gaps in coverage can be seen to bring the noise features up to 1.0 – 2.0 % for arrays depleted in a random fashion down to 18 – 12 elements. However, the basic high-resolution structure in the core of the image remains, albeit somewhat degraded in signal-to-noise. For severely depleted arrays of 9 & 6 elements given in Figure 1 part C, the sidelobes rise to become comparable with the peak. Some of the inner structure survives, however in such cases it would probably be more profitable to fit models to the dataset rather than attempt full imaging.

In order to check the robustness of this result the images in Figure 1 part C (at severe levels of array depletion) were re-done using the CLEAN algorithm as implemented in the AIPS package. The reason for doing this is that we have found that the latter software can provide usable maps under more challenging conditions than our version of MEM. (MEM on the other hand, provides nicer maps with somewhat higher resolution for good data sets). In Figure 2 we show the results of CLEAN mapping, showing that even for the severely depleted arrays down to 9 & 6 elements, maps showing real structure can be obtained. Indeed, the full spiral of the original image is recognizable with a dynamic range approaching 100 based on only 9 array elements.

3. STUDY 2: SYSTEMATICALLY DEPLETED ARRAY

This experiment used identical data to that of Study 1: Wolf-Rayet 104 as mapped from a 36-hole circular ring. In this instance, the array was depleted so as to preserve as much

as possible the uniformity of coverage out to long baselines. Results are given in Figure 3. Again we see excellent imaging performance, with some loss of dynamical range, down to arrays of 18 and 15 elements. As before, more severe degradation is seen for arrays of 12, 9 and 6 elements respectively.

In comparison with the equivalent randomly depleted case (Figure 1), there does not seem to be a marked improvement, although the sidelobes are more uniform and the central structure perhaps a little better preserved. Given the very much larger gaps and rents in Fourier coverage for the randomly depleted case, this near-parity of the two cases was surprising. One reason that we did not see a dramatic improvement might be that the randomly depleted case preserved some of the very short baselines, not kept here, which help to preserve field-of-view. However, it appears that in this instance the non-uniform coverage was not highly detrimental to the imaging process. If this result is found to hold for other cases (and extrapolation on this one result is dangerous), it clearly helps the designers of ground-based interferometers who are struggling to fill the Fourier plane.

As before, we have also used CLEAN to map the severely depleted cases, with results shown in Figure 4. Again, good preservation of the core structure has been found, this time right down to some recovery even with only 6 elements. Note here the higher sidelobes due to the lack of short spacings limiting the field-of-view.

4. STUDY 3: A MORE CHALLENGING CASE

We have experimented also with a more difficult case: IRC +10216 is one of the largest and brightest objects in the infrared sky, and its extended and complex morphology make for a harder job in producing a good image. Observations with a 21-element array yield a good map with a dynamic range of about 100:1. However, as is seen from Figure 5, the image can be seen to rapidly deteriorate as the array is depleted, with most of the useful extended structure having disappeared by the 15-element image, and very little useful structure (even of the elongated core) preserved below 12-elements.

For this image, extended structure covers about 400 mas. For comparison the maps of WR 104 earlier had flux over only about 180 mas. If we assume that the resolution of the primary beam produced in the maps is 40 mas (allowing for some modest super-resolution) then it is interesting to ask approximately how many diffraction-limited beams the maps cover. For IRC +10216 it is about 100, while for WR 104 the number is closer to 20. If we take the rule-of-thumb about the number of visibilities equating to the number of pixels (resolution elements), then we should need (from Table 1) about a 15-element array to observe IRC +10216 and a 7-element array for WR 104. From what we have seen, this would appear not far from the truth (if somewhat optimistic) as with 18 and 9 element arrays respectively we have mapped both of these cases adequately.

5. CONCLUSIONS

Using real interferometry imaging data and artificially depleting the Fourier coverage we have shown that reasonable mapping performance for relatively compact objects can be preserved for low numbers of array elements. For an object with structure of only 4–5 diffraction-limited beamwidths across, images could be obtained with as few as 9–12 elements operating in a snapshot mode. Similar imaging performance might be expected

from an earth-rotation synthesis telescope of some 5-7 elements. For larger objects (in this instance 10 diffraction-limited beamwidths across) more Fourier coverage was needed, with our example requiring 21–18 element snapshot arrays.

TABLE 1. Quantity of Fourier data as a function of number of array elements.

number of stations	visibilities (baselines)	raw closure phases	independent closure phases
3	3	1	1
4	6	4	3
5	10	10	6
6	15	20	10
7	21	35	15
8	28	56	21
9	36	84	28
10	45	120	36
11	55	165	45
12	66	220	55
13	78	286	66
14	91	364	78
15	105	455	91
16	120	560	105
17	136	680	120
18	153	816	136
19	171	969	153
20	190	1140	171
21	210	1330	190
22	231	1540	210
23	253	1771	231
24	276	2024	253
25	300	2300	276
26	325	2600	300
27	351	2925	325
28	378	3276	351
29	406	3654	378
30	435	4060	406
31	465	4495	435
32	496	4960	465
33	528	5456	496
34	561	5984	528
35	595	6545	561
36	630	7140	595

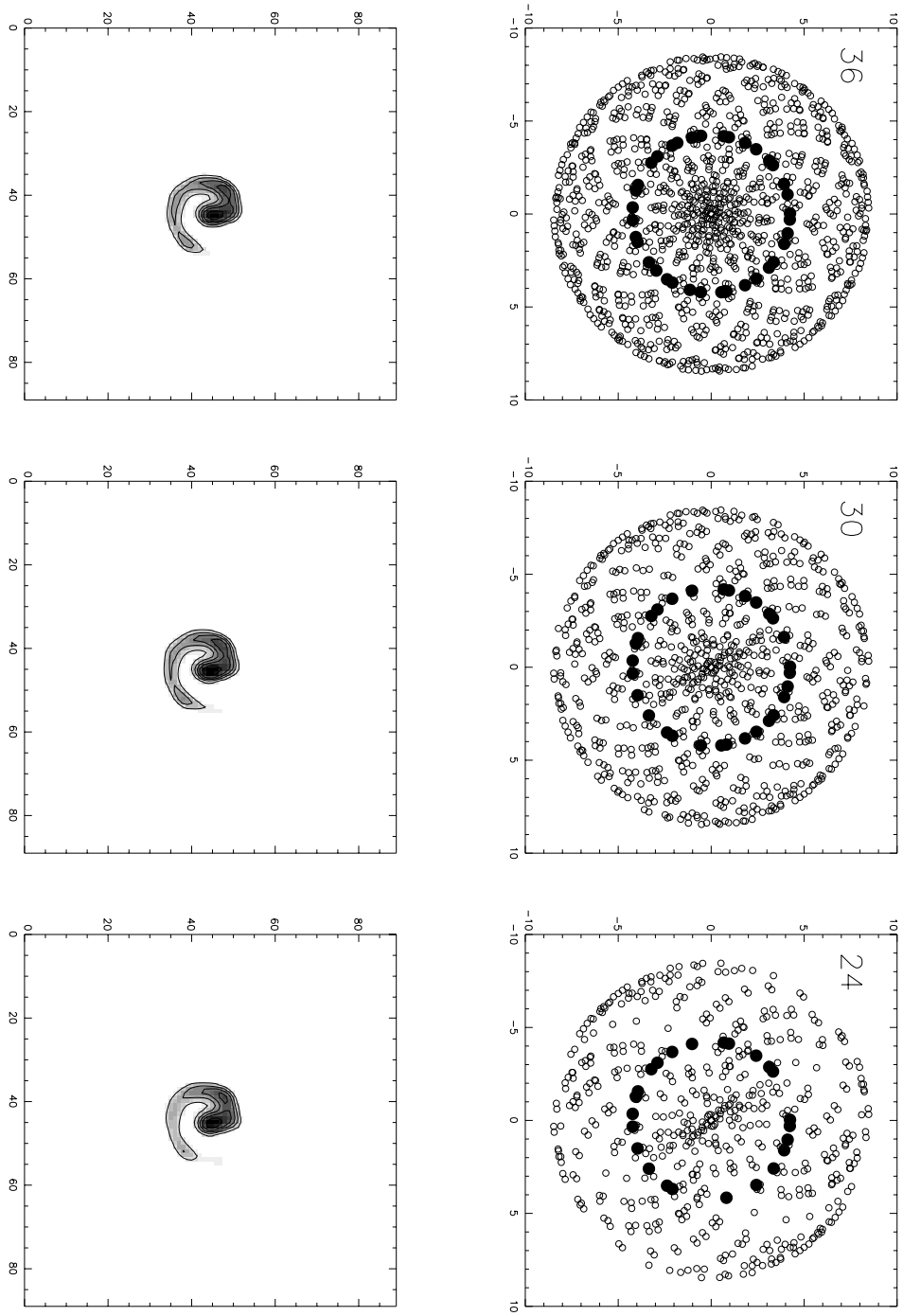

FIGURE 1. PART A. Array Geometries (filled dots) and Fourier Coverage (open circles) for a progressively and randomly depleted array starting with 36 elements. Corresponding images generated by MEM self-calibration are given. Contour levels are 1,2,5,10,20,50 % of the peak. Field-of-view of the images is 630 mas.

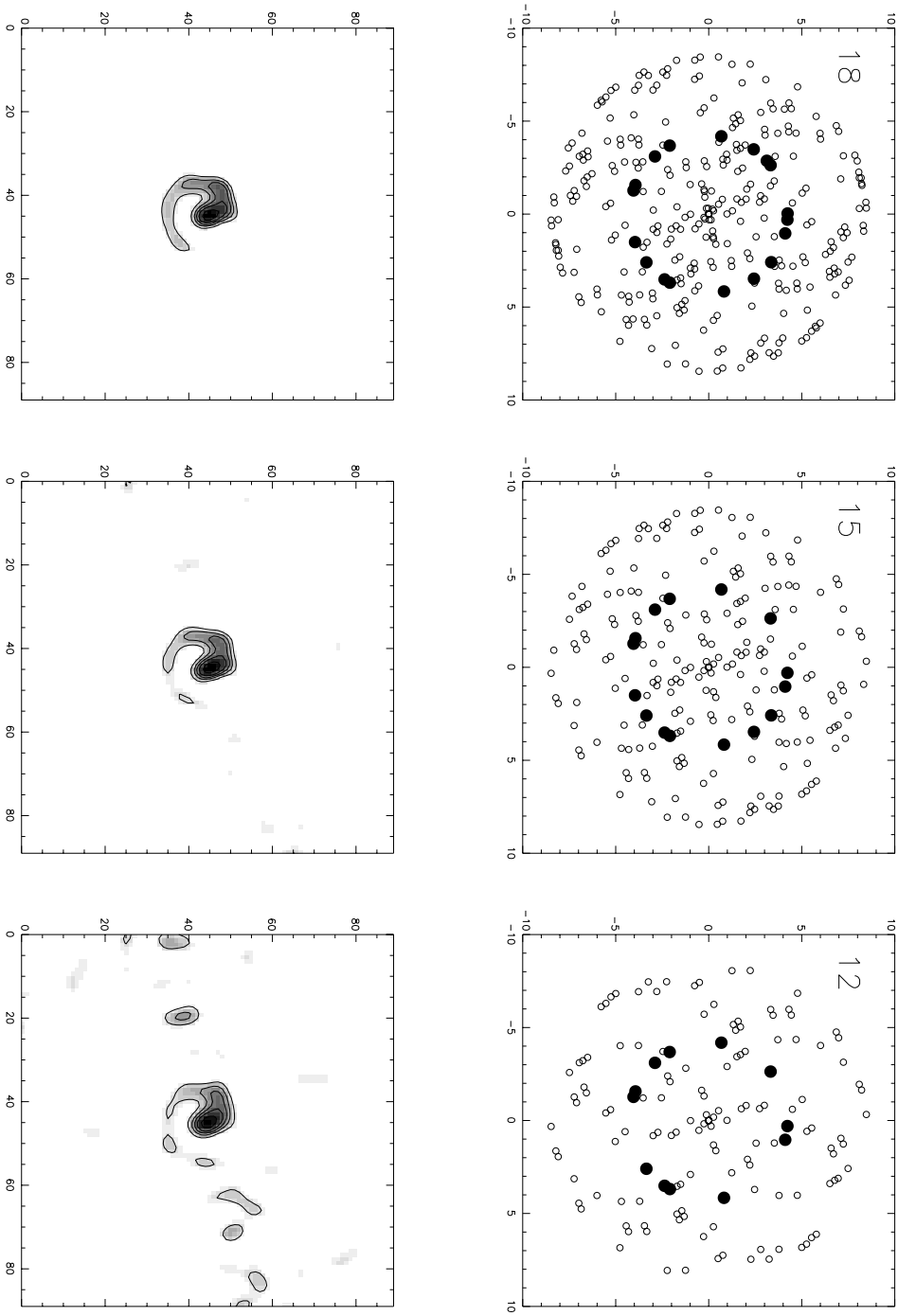

FIGURE 1. PART B. Continuation of Figure.

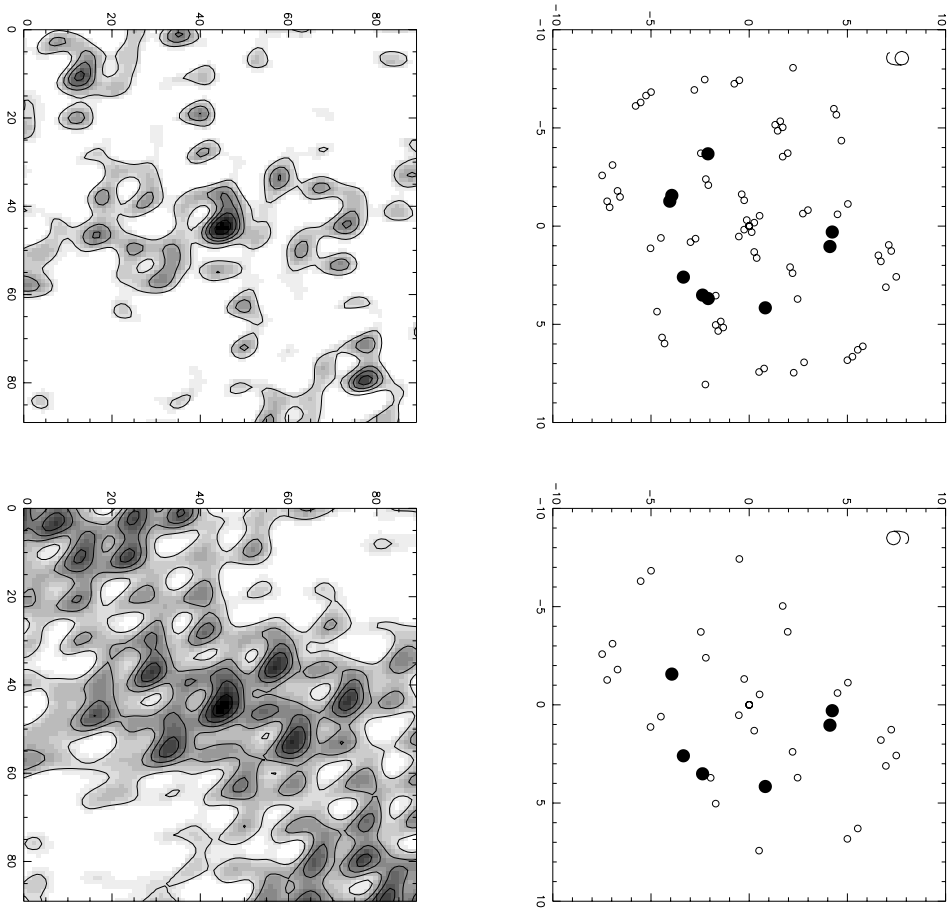

FIGURE 1. PART C. Continuation of Figure.

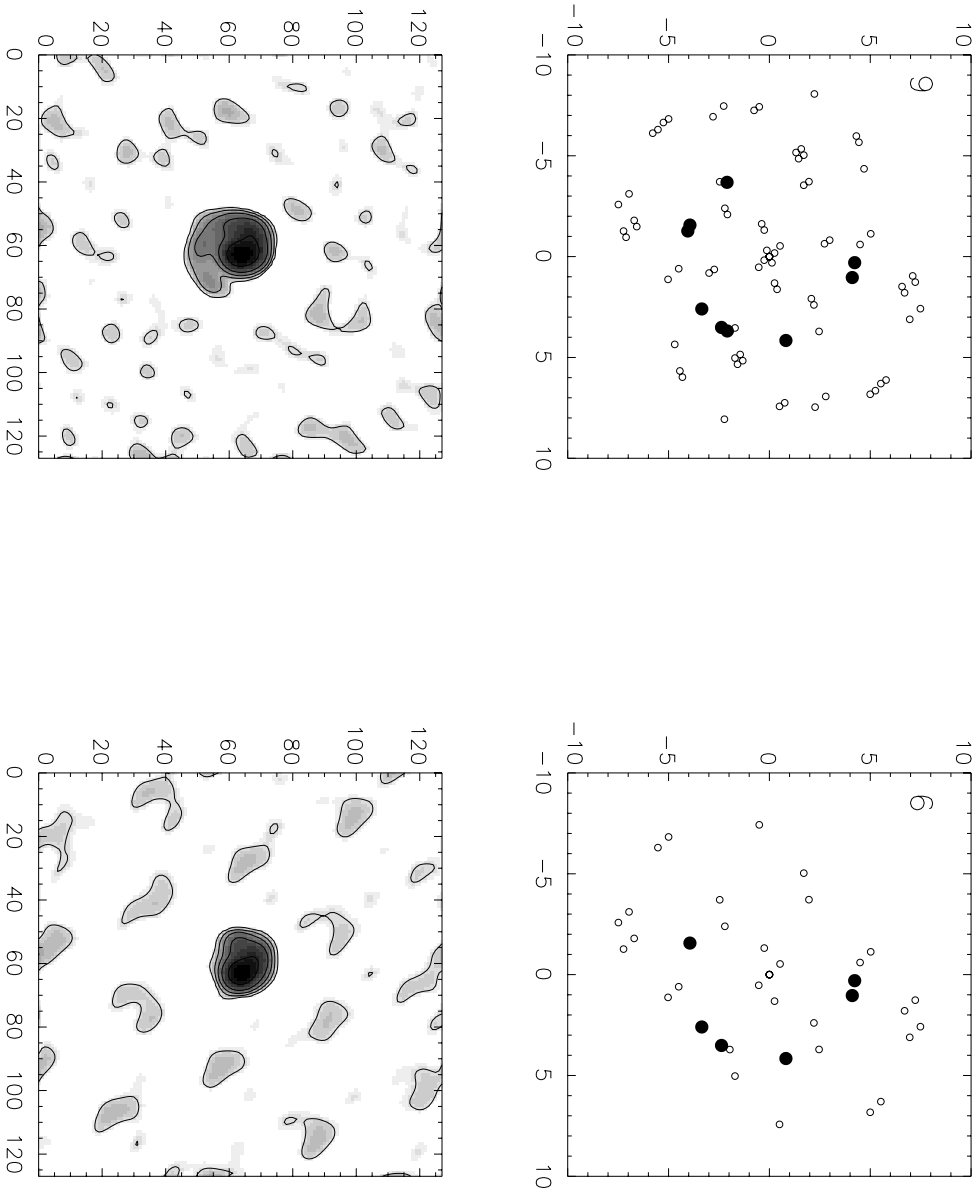

FIGURE 2. Repeat of Figure 1 part C for arrays depleted to 9 and 6 stations. In this instance, the CLEAN imaging algorithm as implemented in the AIPS package has been used for the mapping. As before, contour levels are 1,2,5,10,20,50 % of the peak and field-of-view is 630 mas.

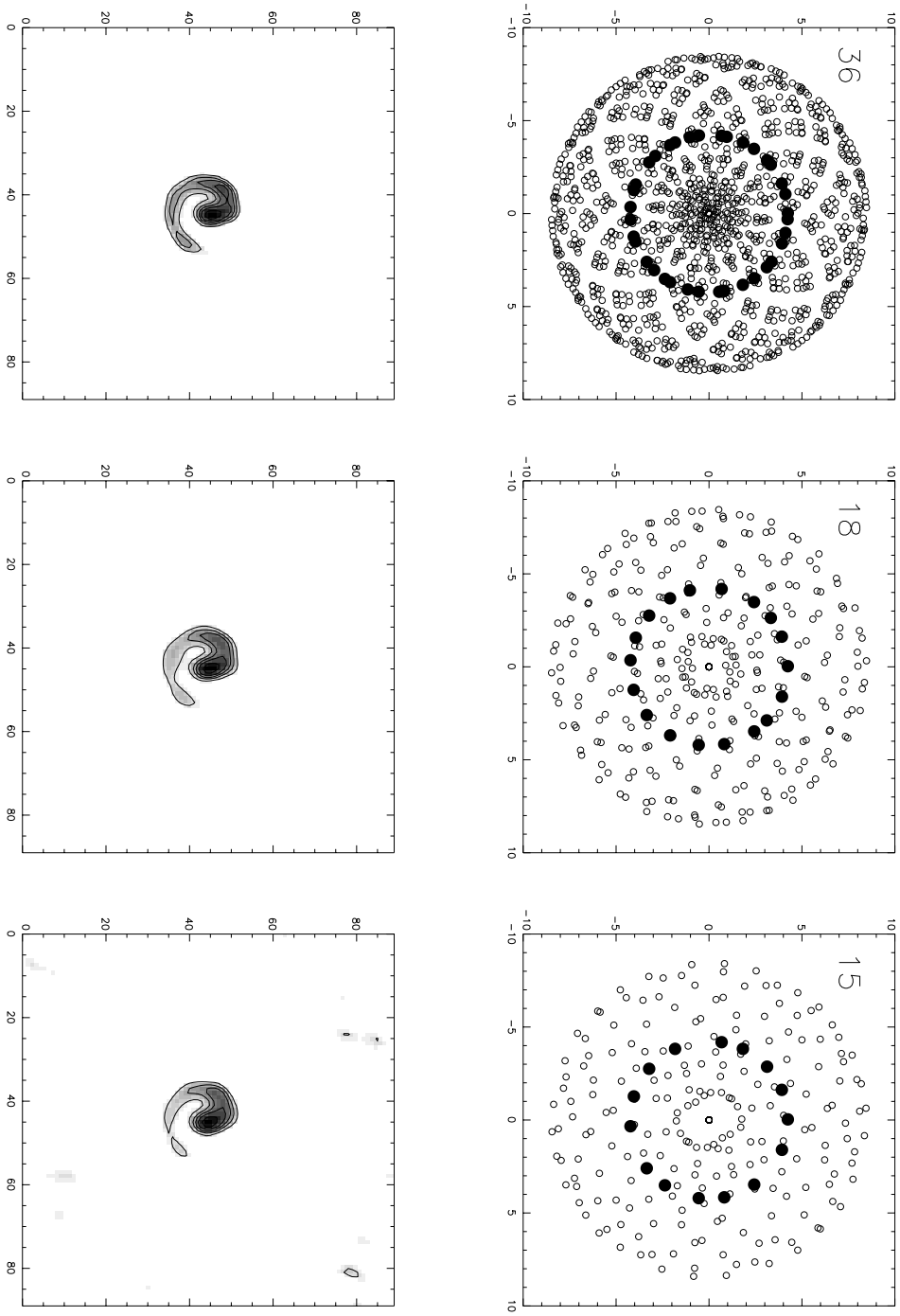

FIGURE 3. PART A. Fourier coverage and images produced from aperture synthesis data on WR 104 as used for Figs 1 & 2. In this instance, the arrays have been depleted in a systematic (rather than random) fashion. Contour levels are 1,2,5,10,20,50 % of the peak and field-of-view is 630 mas.

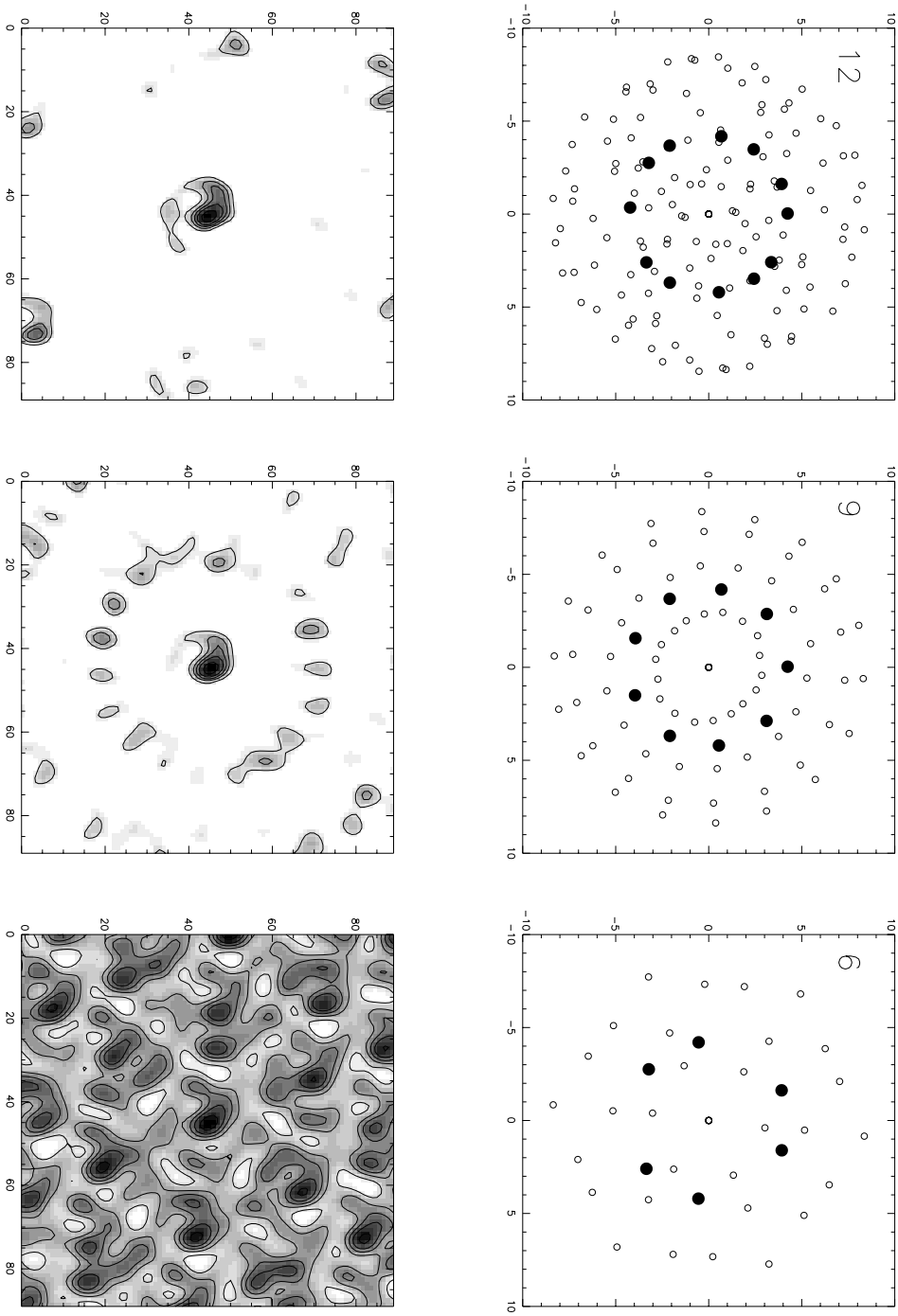

FIGURE 3. PART B. Continuation of Figure

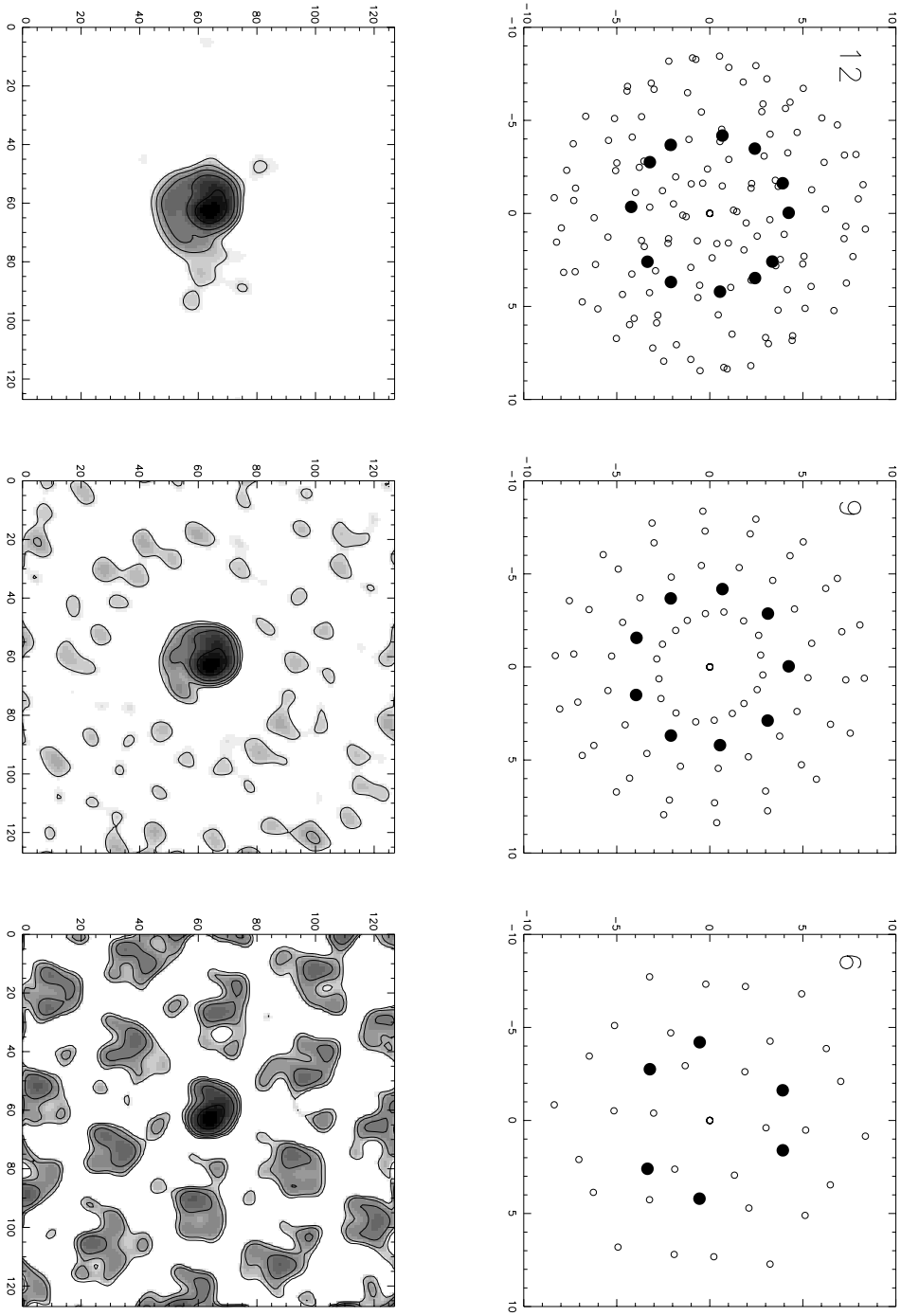

FIGURE 4. Repeat of Figure 2 part B for arrays depleted to 12, 9 and 6 stations. In this instance, the CLEAN imaging algorithm as implemented in the AIPS package has been used for the mapping. As before, contour levels are 1,2,5,10,20,50 % of the peak and field-of-view is 630 mas.

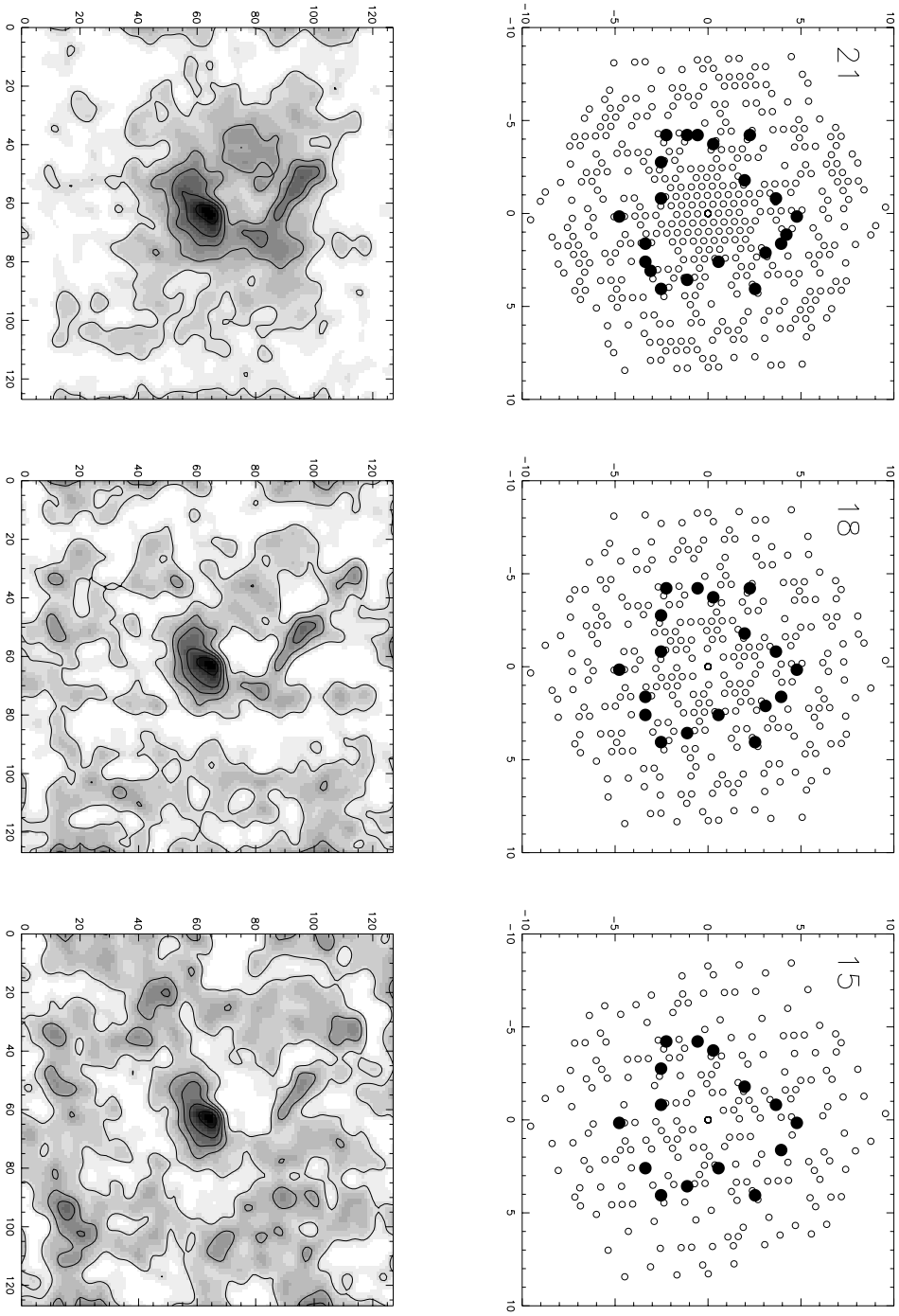

FIGURE 5. PART A. Depletion of Array synthesis data taken on the Carbon Star IRC+10216. The array has been depleted in a quasi-systematic fashion from the original 21-stations. Corresponding images generated by MEM self-calibration are given. Contour levels are 1,2,5,10,20,50% of the peak. Field-of-view of the images is 896 mas.

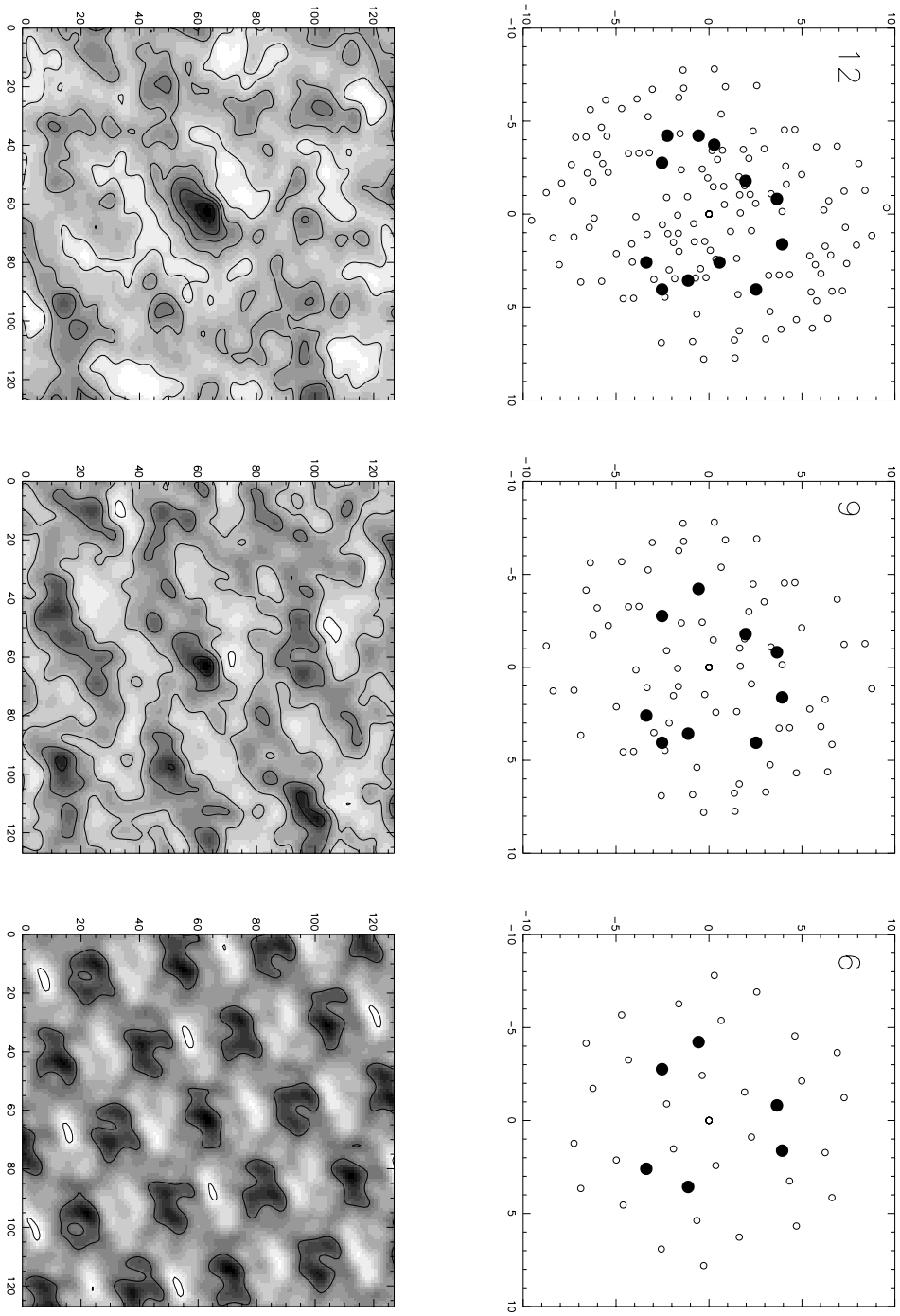

FIGURE 5. PART B. Continuation of Figure.